SSIM 2025 - JJ Potter & J Wesseloo (eds)

doi:10.36487/ACG_repo/2535_54

Threshold assessment of low displacement rates through slow movement analysis

Jorge Calderon [a,*] , Rachael Barnes [b]

[a] *Resource Centre of Excellence, BHP, Australia*

[b] *Decision Science, BHP, Australia*

Abstract

Detecting low-velocity slope movement in open pit mines is vital for early hazard identification and operational risk mitigation. This study explores the use of slow movement analysis (SMA) applied to displacement, velocity, amplitude, and acceleration data from ground-based radar (IDS ArcSAR radars) systems. For a given monitoring area, and across selected time between scans (T) values, statistical and frequency-based features – including those derived from Fast Fourier Transforms – were extracted to characterise slope behaviour.

A hierarchical clustering approach was used to group movement patterns, which were then categorised by geotechnical experts into failure, pre-failure, and stable classes. The analysis included not only failure-related movement but also data from areas showing no signs of instability, allowing for a comprehensive understanding of both indicative and non-indicative movement patterns.

This approach aims to identify consistent feature signatures across failure and non-failure cases and to support the development of interpretive rules that help geotechnical engineers assess whether SMA data predicts failure. The results lay the groundwork for integrating such rule-based insights into predictive monitoring workflows, enhancing safety and decision-making in mine slope management.

Keywords: *slow movement analysis, open pit mining, geotechnical monitoring, ground-based radar, hierarchical clustering, failure detection, feature engineering, Fast Fourier Transforms*

1 Introduction

Geotechnical engineering in open pit mining relies heavily on real-time monitoring technologies to assess slope stability and respond rapidly to high-velocity wall movements. These fast-moving instabilities typically offer lead times on the scale of hours to days, enabling critical interventions that help prevent loss of life. Many publications have addressed the effectiveness of implementation of this type of technology as one of the most effective tools for slope instability management (Abrahams 2023; Read 2009; Hutchinson 2023; Lowry et al. 2013; Sharon & Eberhardt 2020; Crouse & Wines 2016; Yang et al. 2011). While such monitoring is vital for immediate safety, it does not provide sufficient foresight for mine planning, long-term slope management, or broader business continuity activities. For these purposes, the early detection of slow movements – those that may precede failure by weeks or even months – is essential.

Traditionally, detecting and interpreting low-velocity movements from ground-based radars (GBRs) has been a manual and expert-driven process, limiting its accessibility and consistency across operations. Automating the detection and analysis of these slow velocities opens new possibilities for proactive geotechnical risk management. When implemented effectively, such methods can extend the window of warning for impending pit wall instabilities, allowing geotechnical engineers to act earlier and with more confidence.

[*] Corresponding author. Email address: Jorge.JA.Calderon2@bhp.com

The intent of this paper is to support geotechnical practitioners in understanding how to interpret and act on slow movement data. Key questions addressed include when should low-velocity movement raise concern? When is it likely to begin? And when should it trigger intervention? By examining displacement, velocity, amplitude, and acceleration data derived from GBR systems, and applying clustering techniques validated by expert classification, this study identifies recurring movement patterns associated with both failure and non-failure scenarios across various geological settings.

Importantly, not all movement is cause for alarm. In many cases, minor displacements are part of the normal behaviour of a working pit and do not indicate instability. Distinguishing between concerning and non-concerning movement is therefore critical. This paper presents a framework for recognising common characteristics of failure-prone and benign movements, offering a practical guide for assessing when action is – and is not – required. In doing so, it aims to enhance the effectiveness of predictive monitoring and help operational teams make informed, timely decisions based on slow movement analysis.

2 Literature review

Traditional slope monitoring systems such as prisms and the Global Navigation Satellite System (GNSS) network are well-established tools for detecting both rapid and very slow slope displacements, particularly when long-term time series data are available. These instruments provide high-precision measurements and are widely used to validate and track long-term deformation trends. However, GBRs, while highly effective for real-time monitoring of rapid slope movements, are inherently limited in their ability to detect very slow displacement rates, being in the order of millimetres per month. This is because their ability to detect displacement over a time interval (T) is bounded by physical and instrumental constraints:

- The minimum detectable displacement is limited by instrumental noise (i.e. radar electronics) and atmospheric effects (i.e. humidity, temperature changes) which can mask very small displacements.
- The maximum detectable displacement that can be measured between 2 scans is limited by the wavelength of the radar signal. If the displacement exceeds this limit, the radar cannot distinguish between one full phase cycle and another. This upper limit is called phase ambiguity.

In order to detect slower velocities, one needs to increase the time between scans (T), being greater than real-time monitoring time between scans, to allow more displacement to accumulate. This is known as slow movement analysis (SMA), which has emerged as a complementary post-processing technique that aggregates radar data acquired by IDS ArcSAR radars over extended time intervals or greater 'T', thereby enhancing sensitivity to low-velocity movements (IDS Georadar Division Mining 2018) and (Peryoga et al. 2023; Leoni et al. 2015) as it gets closer to Satellite InSAR monitoring, therefore, being able to detect lower displacement rates (Morgan et al. 2019).

SMA has proven particularly effective when integrated with other monitoring technologies such as satellite interferometric synthetic aperture radars (InSAR) and long-term prism or GNSS datasets, forming a multi-sensor framework for comprehensive slope behaviour analysis. Operational case studies have demonstrated the value of SMA in providing early warnings well before real-time radar systems detect any movement. For instance, Peryoga et al. (2023) demonstrated the successful application of SMA at a Rio Tinto iron ore mine, where slow movements were detected months in advance of conventional radar systems. Similarly, Leoni et al. (2015) introduced a multi-scale processing algorithm capable of capturing deformation rates across 4 orders of magnitude, from rapid failures to extremely slow creep. These findings are supported by Venter & Hamman (2019), who emphasised the importance of monitoring frequency and detection delay in managing slope instability risk, and by Saunders et al. (2016), who showed that longer velocity calculation periods significantly improve the detection of slow deformation trends.

Importantly, the early detection of slow displacement rates using SMA may correspond to the initial stages of crack initiation and stable propagation within the rock mass. Eberhardt et al. (1998) along with other authors have identified that brittle rock failure progresses through distinct stages, beginning with microcrack initiation and stable growth, which manifest as subtle volumetric strain and lateral deformation.

These early-stage processes are typically below the detection threshold of real-time radar systems but can potentially be captured through SMA by analysing long-term velocity and displacement trends when there is a slight surface response of that condition. By linking radar-derived physical variables – such as velocity, acceleration, and cumulative displacement – to the mechanical behaviour of rock during crack propagation, SMA provides a valuable tool for identifying the onset of instability (Michelini et al. 2014, 2015, 2019). This integration of geomechanical understanding with advanced monitoring techniques enhances the predictive capability of slope stability programs and supports more informed, proactive decision-making in mine operations (Tovey et al. 2023).

3 Methodology

This study aims to extract actionable patterns from low-velocity slope movement data by analysing time series from IDS ArcSAR radar systems. The approach involves structured feature engineering, unsupervised clustering, and expert classification to inform early warnings for pit wall instabilities.

By doing so, the study seeks to identify displacement trends that may precede failure events, thereby contributing to the development of proactive geotechnical risk management strategies. SMA enables the detection of displacement rates that fall below the sensitivity threshold of real-time monitoring data acquired by IDS ArcSARs, offering a unique opportunity to identify early-stage slope instabilities.

Figure 1 illustrates the methodological framework and sequential processes followed in this study to assess the application of this study.

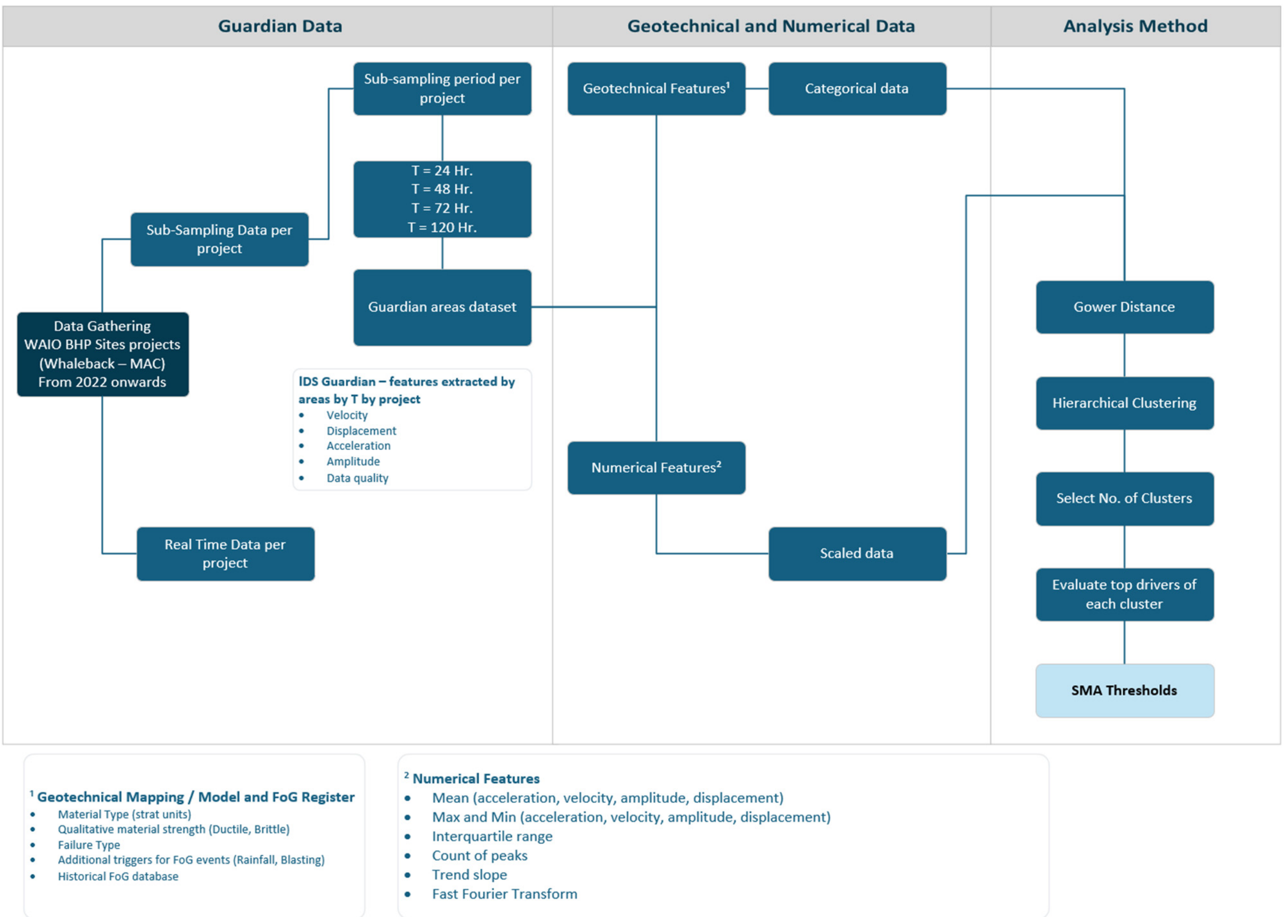

Figure 1 Methodological framework for slow movement analysis thresholds

3.1 Data sources and site selection

The analysis was conducted using historical radar monitoring data from BHP's Western Australia Iron Ore (WAIO) operations, specifically from sites located in the Pilbara region, including Whaleback, South Flank, and Mining Area C (MAC). A total of 18 radar monitoring projects, spanning from 2022 to March 2025, were selected for this study. Each project provided over 3 years of continuous monitoring data, ensuring a robust dataset for back-analysis.

3.2 Analytical framework

A structured, multi-step approach was adopted to implement SMA and analyse the historical data.

3.2.1 Selection of historical projects

Projects were selected based on the availability of radar data capturing known slope failures, supported by complementary geotechnical monitoring records. This ensured the inclusion of both failure and stable slope conditions for comparative analysis.

3.2.2 Slow movement analysis project configuration

SMA projects were created within the monitoring software used by IDS radars (Guardian®) for each of the 18 historical datasets. Multiple time intervals (T) were configured to assess the sensitivity of SMA to different displacement rates. The selected intervals were:

- T = 24 hours
- T = 48 hours
- T = 72 hours
- T = 120 hours.

The rationale for using varying T values is due to GBRs being limited in detecting lower velocities due to the two constraints outlined in Section 2 – the lower displacement limit is masked by instrumentation noise and the upper displacement limit is constrained by the radar's wavelength. This upper limit is called phase ambiguity, where the radar cannot distinguish between full phase cycles. The higher T values in the list above measure the time between scans, giving more time for the minimum displacement to have accumulated. The instrumentation accuracy can be determined by the following equation:

$$\Delta\varphi = \frac{4\pi\ \mathrm{d}}{\lambda} \tag{1}$$

where:

$\Delta\varphi$ = phase difference between 2 consecutive acquisitions

d = distance difference between 2 consecutive acquisition relative to radar position.

λ = wavelength of the electromagnetic signal sent by the radar (Ku band for ArcSAR radars).

For this application, the plot was developed using Ku band, which is the wavelength of IDS ArcSAR radars, considering that the information was taken using IDS radar units (ArcSARs). Longer T intervals enhance the detection of slower movements but reduce the ability to capture higher velocities.

While increasing the time between scans (T) enhances sensitivity to slow movements, it also introduces challenges – particularly if a stable reference frame is not well defined. Over longer intervals, small errors in radar positioning, atmospheric variations, or ground reference drift can accumulate, leading to poorer data quality and reduced reliability in displacement measurements. This was handled by discarding any data below a certain data quality threshold and taking measurements in multiples of 24 hours apart from the early hours in the morning. This minimises atmospheric disturbances and ensures data is collected in roughly the same temperature and atmospheric conditions at the same time of day. Additionally, shorter T intervals are more suitable for detecting rapid displacements. A log-log plot illustrating the velocity detection range across different T values is included to support this concept in Figure 2. The upper and lower bounds (see minimum and maximum velocity lines) for the velocities for each T value are theoretical in this graph – variations in practice will occur due to instrumentation error and atmospheric changes over time.

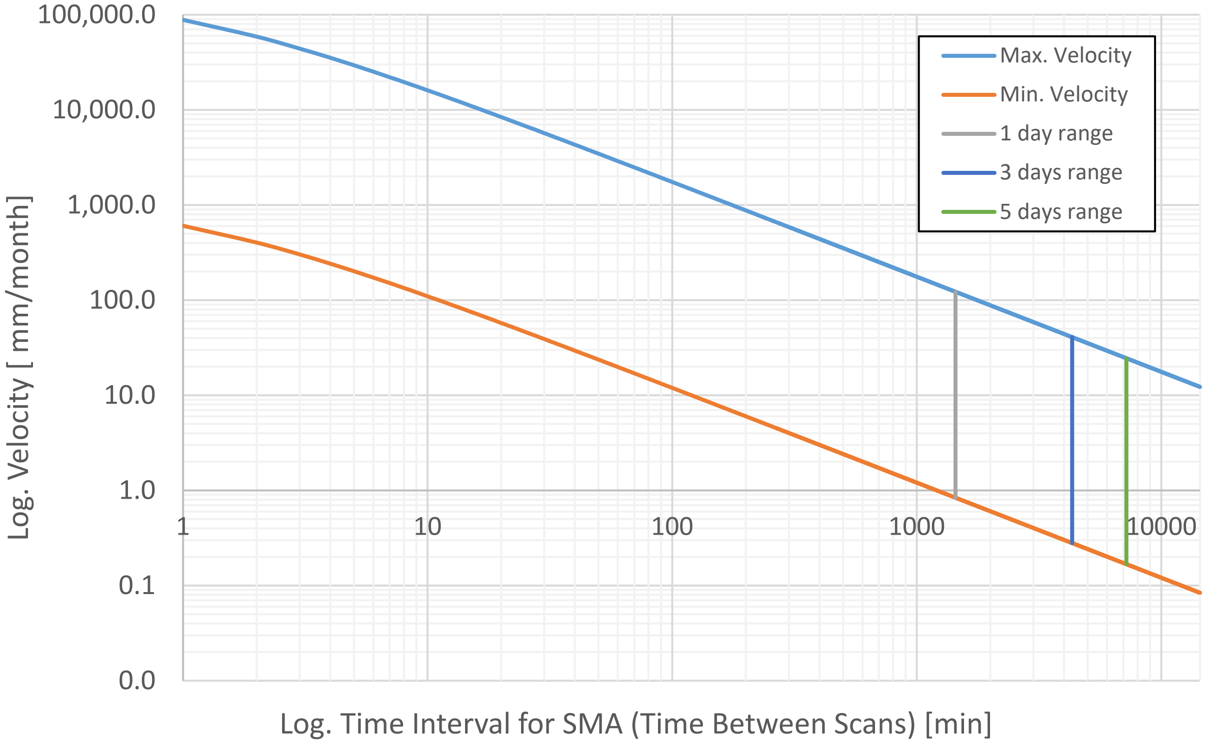

Figure 2 Detectable displacement rates by time interval

In total, 72 SMA projects were generated (18 sites × 4 T values), forming the basis for subsequent analysis. The analysed data considers T values of 1, 2, 3 and 5 days as T values to acquire velocities in the range of 0.1 to 1 mm/month.

3.3 Definition of analysis areas in Guardian®

Within each SMA project, specific areas were delineated based on the following criteria:

- Integration of geotechnical features such as major faults, stratigraphic unit contacts, and detrital boundaries, which are known to influence slope behaviour.
- Identification of zones with documented historical failures, ensuring spatial correlation with geological structures.
- Delineation of stable zones for baseline comparison.
- Detection of areas exhibiting slow displacement under SMA, including those extending beyond known failure zones. Previous studies have shown that SMA can reveal broader zones of slow movement surrounding the core failure area, with the extent of these zones varying by T value. Larger T intervals (e.g. 120 hours) are expected to capture more extensive areas of low-rate displacement.

For each defined area, key parameters were extracted from Guardian, including:

- displacement
- velocity

- acceleration
- amplitude
- data quality metrics.

The following figures illustrate a comparative visualisation of a radar monitoring project in three configurations:

- Figure 3: a standard real-time view using typical colour bar settings. Usually, during real-time monitoring, a short time window is defined in order to evaluate displacements in the range of days and hours. In this example, the radar view is defined by 10 millimetres in a time window of 3 rolling days.
- Figure 4: a forced visualisation of the entire dataset using real-time data. This information helps to understand all the geotechnical events picked up by the radar during the time period of the radar project.
- Figure 5: an SMA view. The SMA visualisation clearly reveals areas (highlighted in red) of slow displacement that are not readily apparent in the standard or forced real-time views.

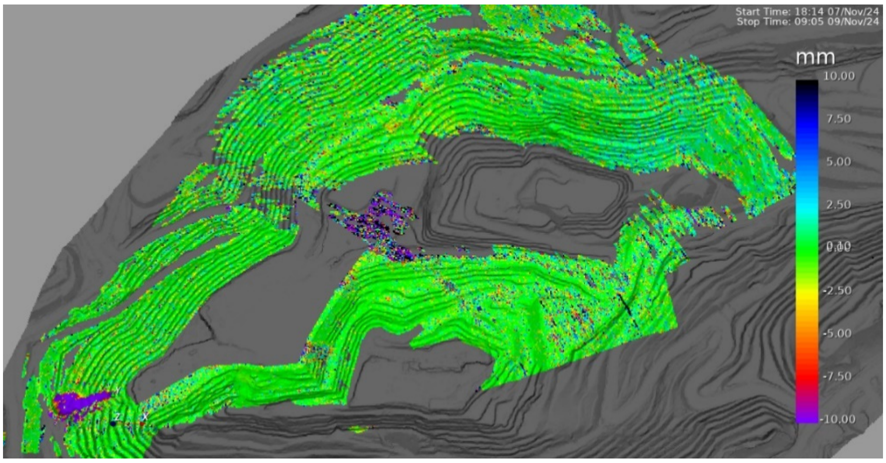

Figure 3 A standard real-time radar view considering 10 mm min./max. cumulative displacement for the last 3 days

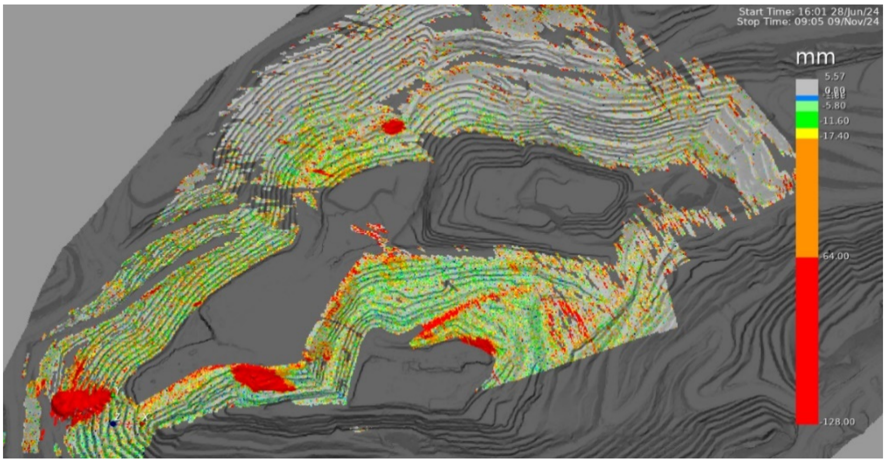

Figure 4 Cumulative displacement radar view for the whole time frame of the real-time project, considering 128 mm as maximum displacement over that time frame

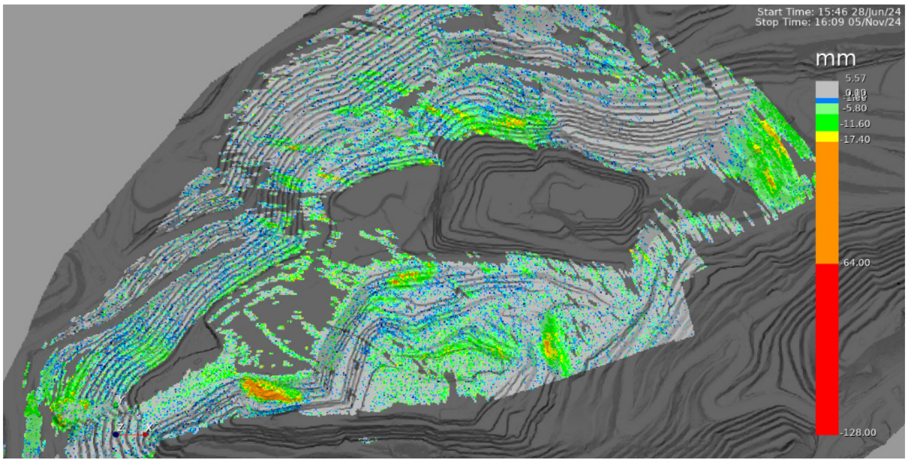

Figure 5 Radar view for slow movement analysis where areas with slow displacements are visible

Areas of interest were defined using both real-time monitoring data and SMA outputs. In particular, regions exhibiting anomalous displacement patterns in the SMA view – yet not flagged in real-time – were delineated as potential zones of concern. This dual approach to area definition enhances the interpretive value of SMA by integrating it with operational real-time insights, allowing for the identification of subtle, early-stage movements that may otherwise go undetected.

3.4 Dataset compilation

A comprehensive dataset comprising over 2,000 individual areas was compiled. Each entry included the extracted parameters and was categorised based on the geotechnical context and SMA configuration.

3.5 Data structure and preprocessing

The dataset was organised at a granular level defined by each project, timescale (T, or time between scans), area (A), and data type – where the data types include velocity, acceleration, displacement, and amplitude. For each unique combination of project, T, A, and data type, a time series was available.

To represent each time series numerically, a suite of features was computed:

- Mean, standard deviation, maximum, minimum, interquartile range.
- Trend slope: average rate of change across the time series.
- Number of peaks: defined as values exceeding one standard deviation above the mean, to avoid false positives from noise.
- Dominant frequency: computed using the Fast Fourier Transform, capturing the most significant periodic behaviour in Hertz (Hz).

To ensure comparability, all numerical features were scaled to prevent domination by higher-magnitude metrics.

3.6 Integration of geotechnical features

Geotechnical attributes were appended to each area in the dataset, enabling correlation between displacement behaviour and geological/geotechnical conditions. This facilitated a more nuanced interpretation of SMA outputs in relation to site-specific geotechnical features.

Additional categorical variables were appended to enrich the dataset:

- Rock mass type: this feature was incorporated using a simplification of the actual stratigraphic units defined in WAIO sites. The criteria for this simplification considers similar rock mass behaviour (in terms of rock mass strength) and the main drivers for its failure mechanisms. The analysed rock mass types, also known as material type for clustering purposes, are ACS3S, detrital, D-R contact, OC, S, and W.

- Failure state: labelled as no failure, pre-failure, failure, or post-failure based on fall of ground register.
- Failure type: such as bedding control, rock mass, structural control, or no failure based on fall of ground register.

The Figure 6 shows the stratigraphical units information from the block model in the current topography, which has been one of the main guidelines to define areas in Guardian

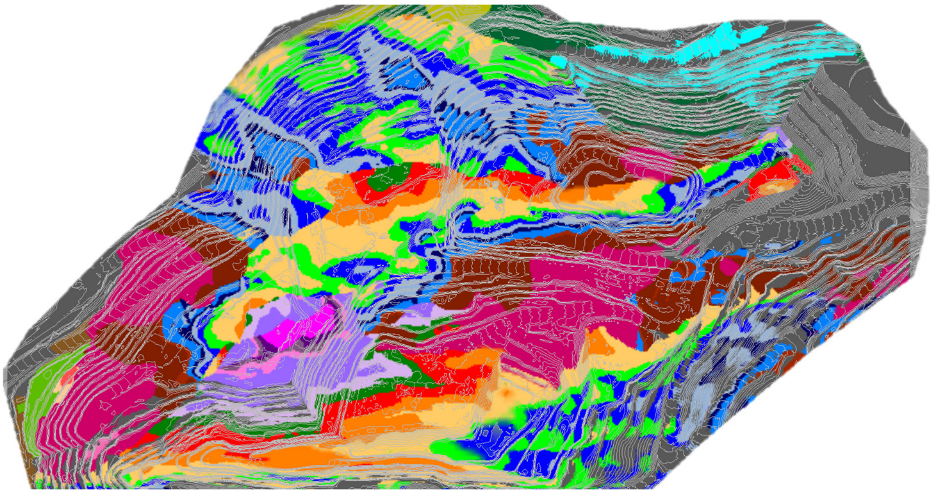

Figure 6 Stratigraphical units visualisation where the geotechnical features were added into the analysis for Mount Whaleback mine (courtesy WAIO Geotechnical Team)

This combined dataset, with both numerical and categorical features, was suitable for mixed-type distance measurement using the Gower distance metric.

3.7 Clustering approach

To group similar movement behaviours, hierarchical agglomerative clustering (as opposed to the other forms of hierarchical clustering, being 'divisive') was chosen over other, typical clustering methods. Unlike these other methods that require a predefined number of clusters or are sensitive to noise and density assumptions, hierarchical clustering is well-suited for uncovering nested patterns. Most importantly, this form of clustering can reveal structure even when not all the features contribute. For example, a failure may not be due to material properties, but due to the contact between different stratigraphic units; this means that the material features would not have been driving the clustering for that instance. This allows for a more flexible exploration of the data structure, especially when the number and nature of clusters are not known in advance. This is particularly important in geotechnical contexts, where the causes of failure are not necessarily known beforehand.

Of note, the features were both categorical and numerical, which required Gower's distances to convert the dataset into something that can be clustered. Gower's distances calculates the similarity between each of the different pairs of data points (each point has its displacement, velocity, geotechnical features, and others, assigned to them) . Between two data points, a similarity score is calculated for each of the features, where categorical variables are assigned '1' if the same or '0' if not. For numerical variables, the similarity for a feature between data points 'I' and 'j' is

$$similarity_{numerical} = 1 - \frac{|x_i - x_j|}{range\ of\ feature} \quad (2)$$

The final similarity score, S_{ij}, between pairs of data points ('I' and 'j') is the weighted average of the similarity calculations. The Gower's distances themselves are calculated with the following formula:

$$Gower's\ distance = \sqrt{1 - S_{ij}} \tag{3}$$

Replacing the original dataset is a distance table showing effectively how 'different' (hence 'distance') between each pair of data points. It yields an $n \times n$ matrix of values between 0 and 1, which is then used as the input into the hierarchical clustering method just described (the main diagonal is effectively 'null', as a distance between a point and itself is not a required calculation).

The hierarchical clustering was also applied using the Ward.D2 method (Murtagh & Legendre 2011). The Ward.D2 method is deemed the most suitable out of all the hierarchical clustering methods as it is sensitive to subtle changes in variables (i.e. displacement) over time, while also being able to find the meaningful information in the data among the inherent noise (such as from atmospheric effects). The hierarchical clustering method was selected due to its effectiveness in minimising intra-cluster variance and producing compact, well-separated clusters – an important consideration when subtle changes in movement patterns could signify material differences in geotechnical outcomes.

Clustering was essential to identify naturally occurring groupings that reflected similar movement shapes or behaviours. This process relies on the assumption that failures occurring in similar material types and conditions will exhibit comparable time series signatures for displacement and related physical measures.

The output of hierarchical clustering is a dendrogram, as shown in Figure 7. This tree-like diagram visualises the relationships between the data points based on their similarity (as per the calculations made for Gower's distance). Each branch of the 'tree' is a cluster and the height at which branches merge indicates the dissimilarity between them (each data point sits at the bottom of the diagram). A horizontal cut can be made across the 'branches' to choose the number of clusters. The number of clusters chosen was 10 to reflect the real-world diversity of failure mechanisms across the chosen material types while minimising the chance of overfitting (in overfitting, patterns found are based on random noise, not necessarily on the actual patterns that need to be found). This was deemed a reasonable number of clusters to still create meaningful geotechnical groupings (e.g. failure movement in detritals).

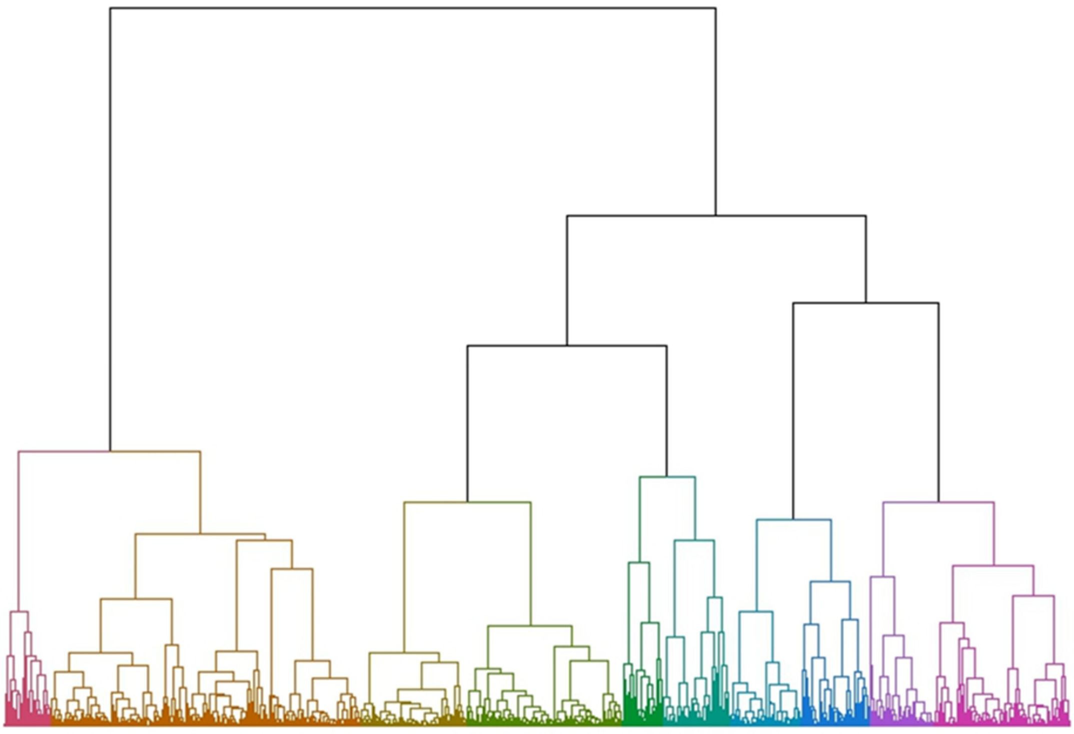

Figure 7 The hierarchical clustering tree or dendrogram which shows the groupings and the relationships between the data points based on their 'closeness' or similarity

3.8 Cluster characterisation and trend extraction

Each observation (defined by project, area, and T) was assigned a cluster and linked to material, failure state, failure type, area name, and derived metrics such as:

- Maximum displacement.
- Elapsed time.
- Displacement rate: calculated as maximum absolute displacement divided by elapsed time.
- Area classification: categorised as small (<8,600 m²), medium (8,600–25,000 m²), or large (>25,000 m²).

The dominant trend in each cluster was typically the displacement slope, which became a key distinguishing factor across failure stages.

3.9 Visual and statistical validation

To further interpret the clusters, **boxplots** of displacement rates were constructed and grouped by material type and ordered by failure stage (pre-failure → failure → post-failure). Only 'pure' clusters (e.g. those dominated by a single failure state) were used for further statistical analysis to ensure the behaviours were not confounded.

Two non-parametric tests were applied:

- Kolmogorov–Smirnov test (KS) and Wilcoxon rank-sum test to test for distributional differences between failure states, under the null hypothesis that distributions are identical.
- For robust threshold setting, median absolute deviation (MAD) was used instead of standard deviation, as it is less sensitive to outliers and does not require assumptions of normality.

Using the MAD, a practical cutoff threshold was derived by subtracting the MAD from the median, informing when movement should trigger closer monitoring for a given rock mass type.

4 Results

This chapter presents the outcomes of the clustering analysis and statistical validation conducted on the compiled SMA dataset. The results are structured to reflect the relationships between cluster groupings and geotechnical characteristics, including material type, failure type, and failure state.

4.1 Clustering outcomes

The hierarchical clustering approach, using the Ward.D2 method and Gower's distance metric, enabled the identification of critical variables influencing slope behaviour across different geotechnical contexts. By grouping areas with similar time series signatures, the analysis revealed:

- Distinct displacement trends associated with specific failure mechanisms.
- Consistent signal patterns within clusters dominated by a single material or failure type.
- Meaningful differentiation between stable and unstable areas, even in the absence of prior failure labels.

Ten clusters were chosen and were evaluated based on their composition in terms of:

- Material type (e.g. ACS3S, detrital, D-R contact, OC, S, and W)
- failure type (e.g. bedding control, rock mass, structural control, or no failure)
- failure state (e.g. no failure, pre-failure, failure, post-failure).

Figures 8, 9 and 10 show these 10 clusters along the x-axis, coloured by material, failure type and failure state respectively. Where one colour tends to represent one cluster, it is an indicator that the ‘colouring’ variable is at least one of the features driving the cluster (there are the similarities between the elements of the grouping). For example, cluster 5 has a distinct ‘pre-failure’, ‘material: dr’, bedding control failure state.

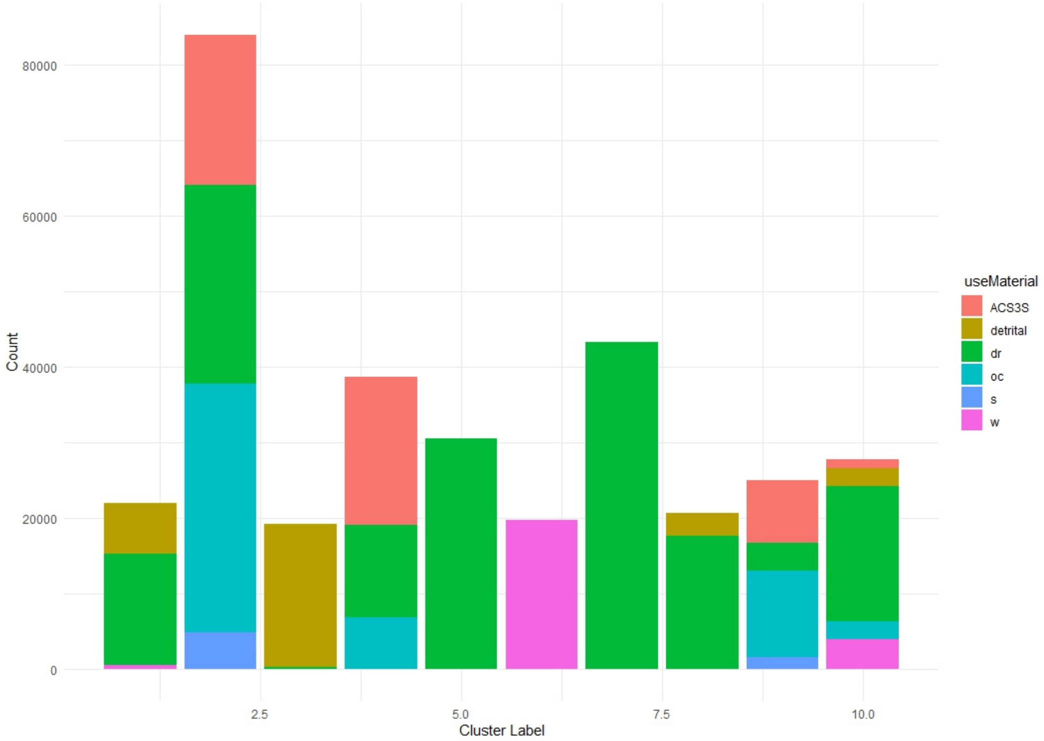

Figure 8 Stacked bar chart by cluster by material type

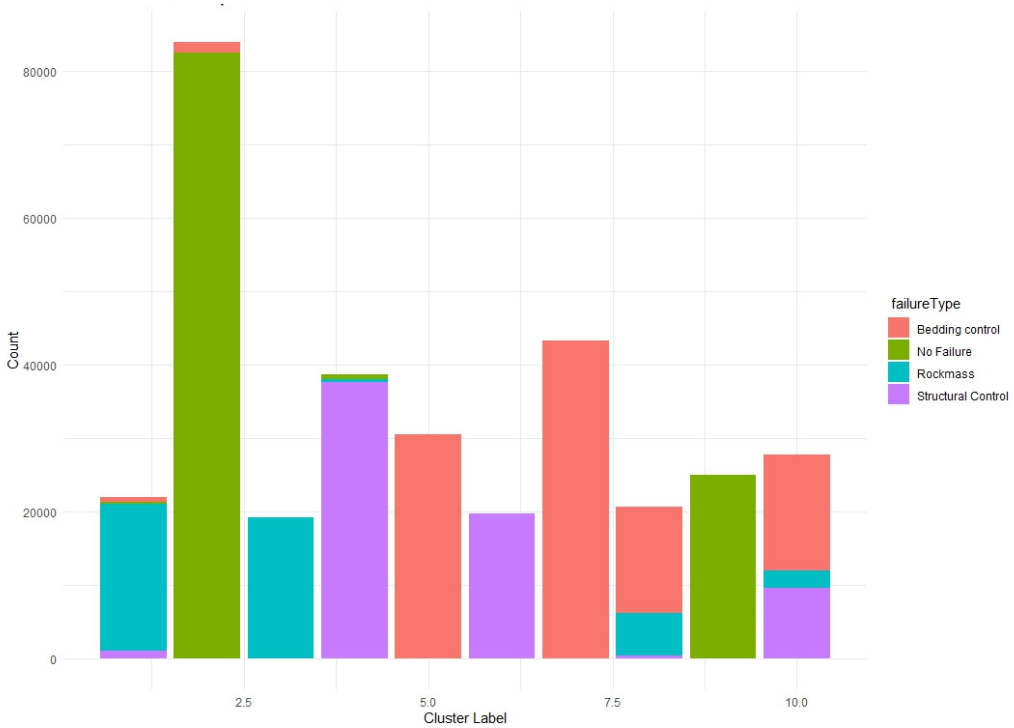

Figure 9 Stacked bar chart by cluster by failure type

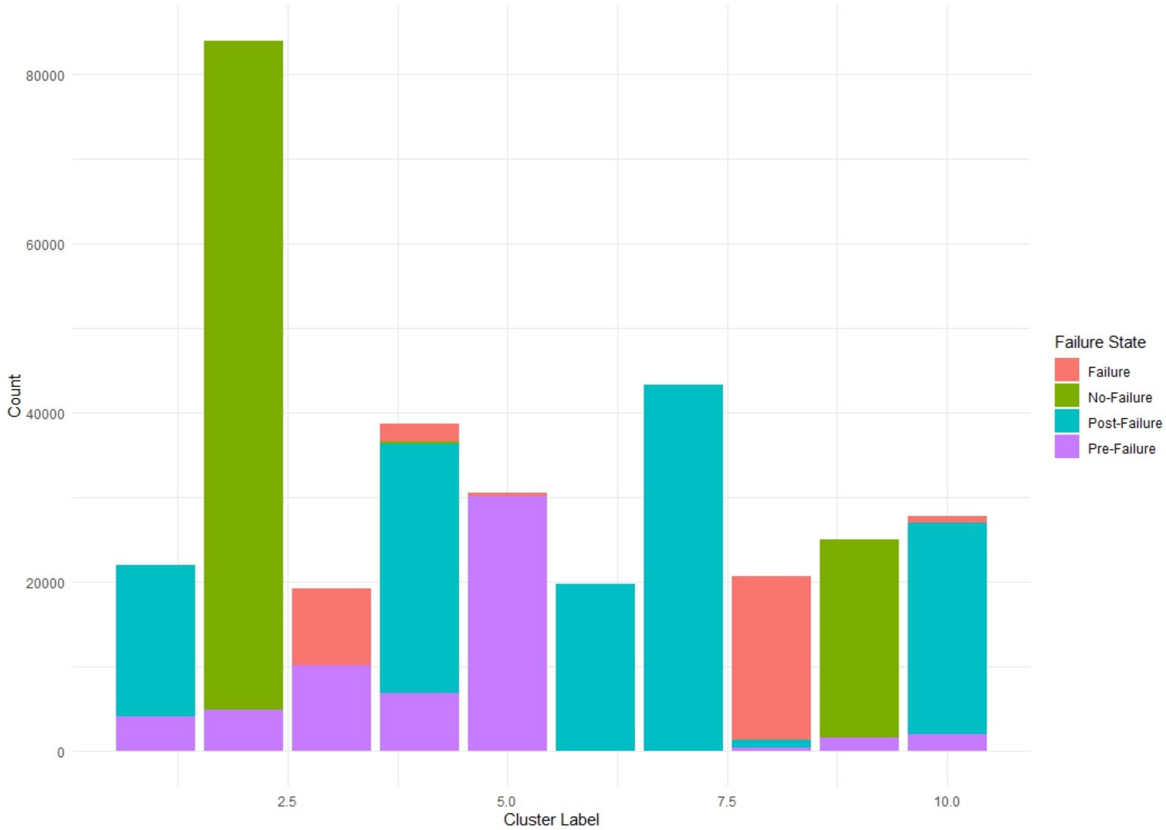

Figure 10 Stacked bar chart by cluster by failure state

The clustering results demonstrated a strong alignment between cluster membership and material type in most cases. Materials such as ACS3S, detrital, D-R contact, OC, S, and W exhibited well-defined clustering patterns, indicating that the SMA-derived features effectively captured the underlying geotechnical behaviour.

However, two clusters – Cluster 2 and Cluster 4 – did not show a dominant material type. Upon further inspection, these clusters were found to be coherent when analysed through other geotechnical lenses:

- Cluster 2 was predominantly composed of areas classified under the 'no failure' state. This suggests that the movement patterns in this cluster represent background or benign displacement behaviours, which are not strongly influenced by material type.
- Cluster 4 exhibited a clear association with structural control as the dominant failure mechanism. This aligns with the 'failure type' classification and supports the hypothesis that structural features, rather than lithological properties, are the primary drivers of displacement in these areas.

These findings reinforce the importance of integrating multiple geotechnical dimensions when interpreting SMA data. While material type is a strong predictor of displacement behaviour in many cases, failure mechanisms and states provide critical context for understanding anomalies or outliers in the clustering results.

4.2 Interpretation of cluster characteristics

This unsupervised learning approach proved effective in uncovering latent structures in the data, offering a data-driven framework for early warning and risk prioritisation in slope monitoring by geotechnical features.

To further interpret the clustering results, a statistical analysis was conducted on the key displacement-related variables across all clusters. This analysis aimed to validate the geotechnical relevance of the clusters and to identify meaningful behavioural patterns associated with different failure mechanisms, material types, and area sizes.

Figure 11 illustrates the relationship between clusters and geotechnical features, highlighting how material type, failure state, and failure mechanism align with the observed displacement behaviours.

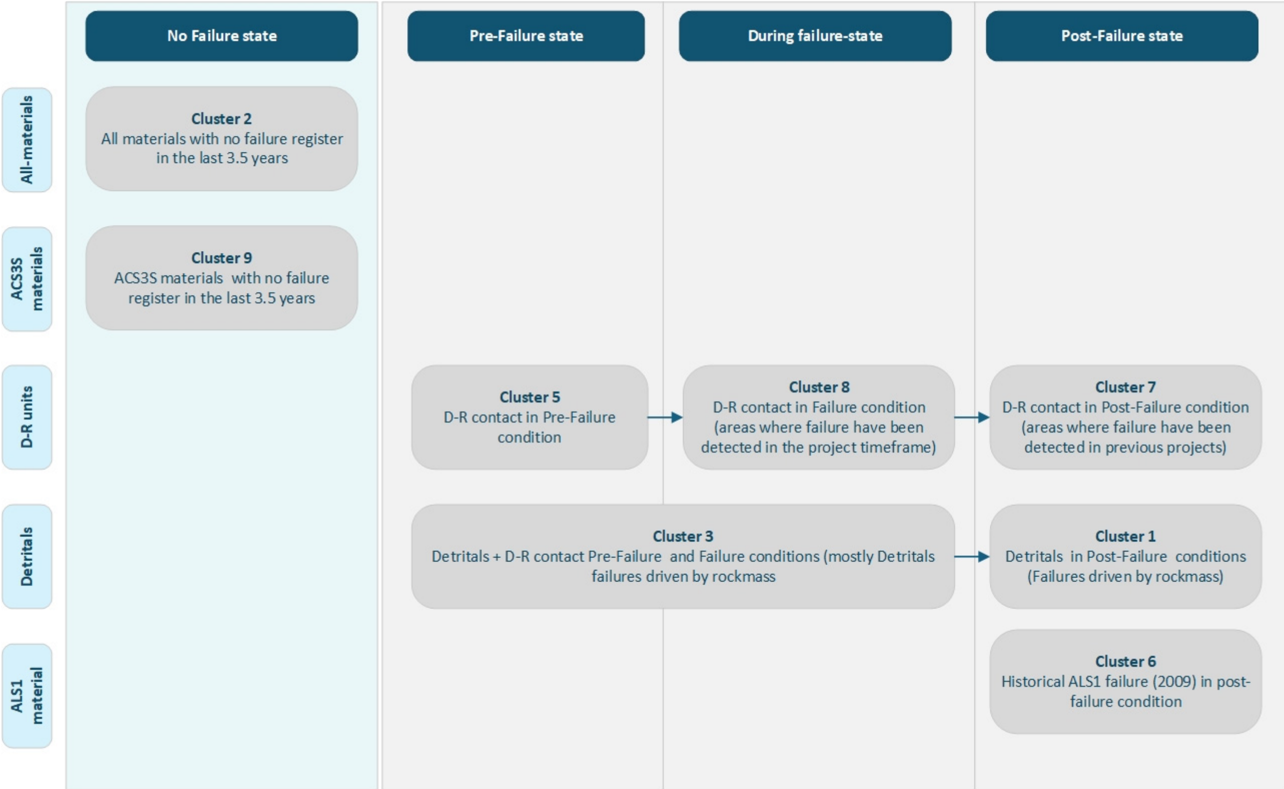

Figure 11 Cluster result by geotechnical features

As outlined in Section 3.3, the areas were defined based on geotechnical and structural criteria, resulting in a dataset with varying area sizes. To avoid analytical bias, the statistical evaluation was stratified by area size – particularly distinguishing between large areas (typically associated with T = 120 hrs) and smaller areas (often linked to T = 24 hrs and real-time failure zones).

4.3 Displacement rate trends by cluster

Figures 12 and 13 present the distribution of displacement rates across clusters, segmented by area size and material type.

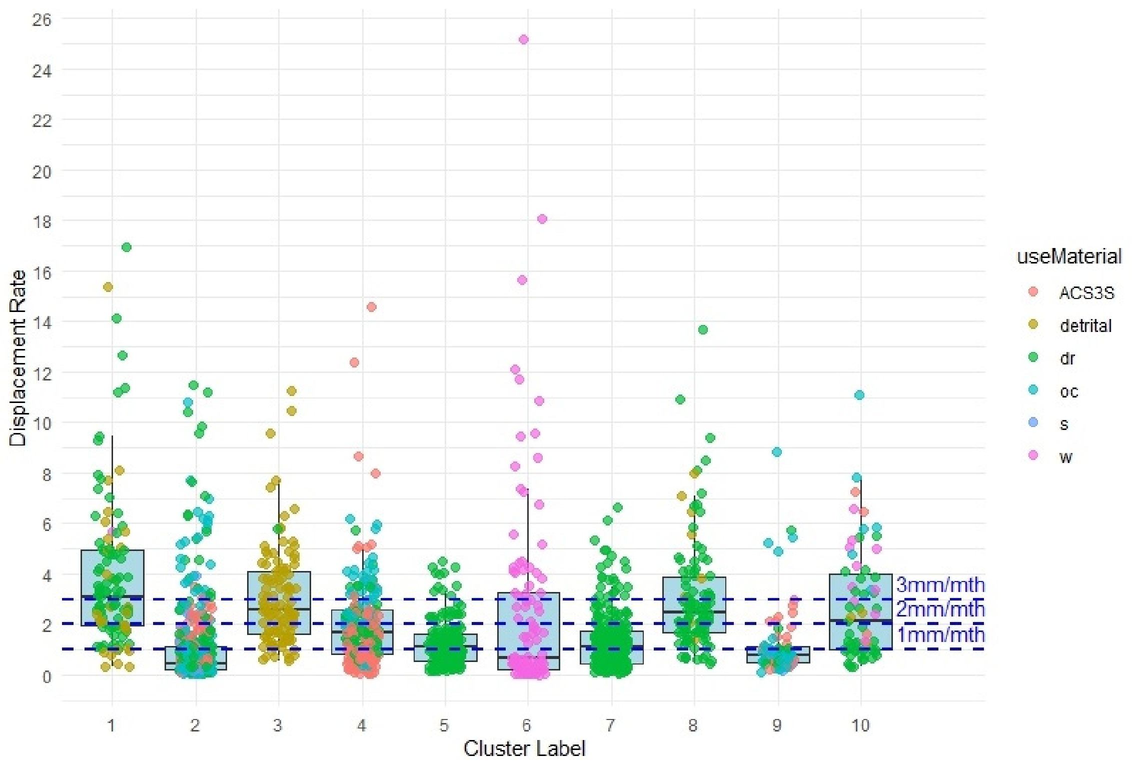

Figure 12 Displacement rate per cluster per material type

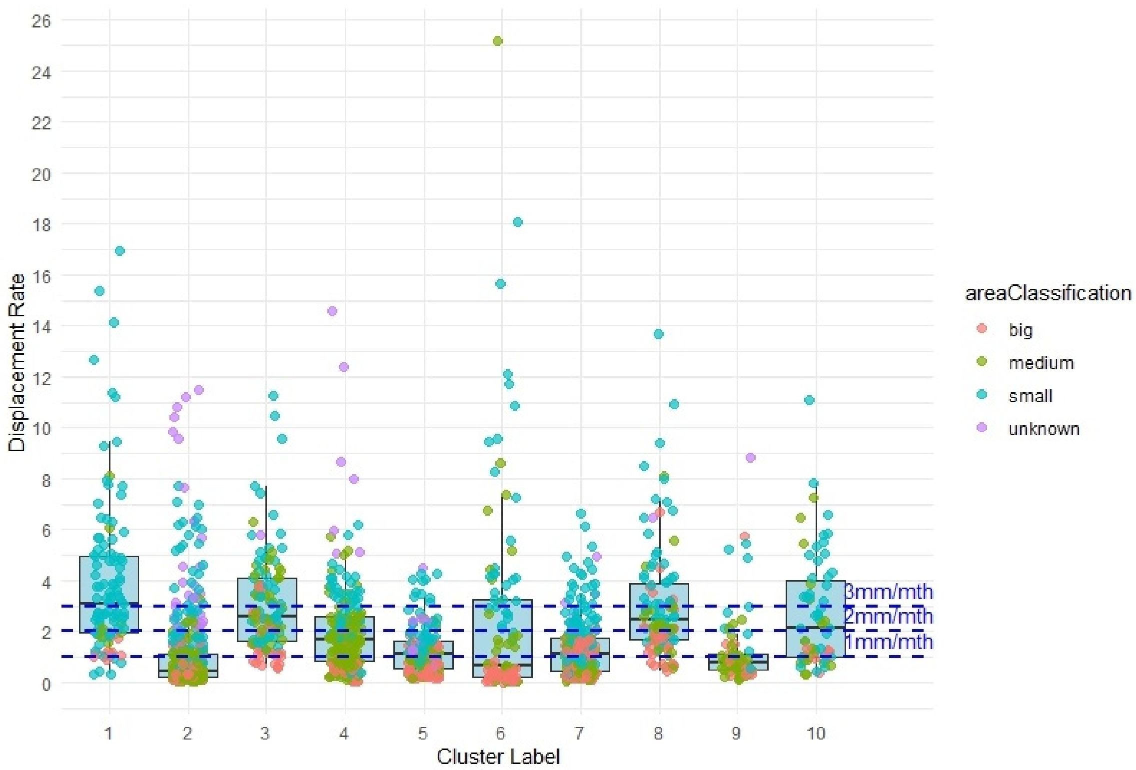

Figure 13 Displacement rate per cluster per area size

The following key observations were derived from the boxplot analysis:

4.3.1 D-R contact materials with bedding control

Clusters 5 and 8 represent distinct failure stages within D-R contact materials:

- Cluster 5: predominantly associated with pre-failure conditions. Displacement rates are generally low, with a mean of 1.4 mm/month, and most values fall below 3 mm/month.
- Cluster 8: represents areas where failure occurred during the radar monitoring period. The median displacement rate is 2.8 mm/month, with several areas exceeding 5 mm/month.

This contrast supports the hypothesis that SMA can differentiate between pre-failure and active failure conditions in bedding-controlled D-R contact zones.

4.3.2 Detrital materials with rock mass control

As expected, due to the ductile nature of detrital materials, the distinction between failure stages is less pronounced:

- Cluster 3: includes both pre-failure and failure states, with a wide range of displacement rates averaging around 3 mm/month.
- Cluster 1: represents post-failure conditions. The displacement rates remain within a similar range, suggesting a gradual transition rather than a sharp behavioural shift.

This finding aligns with the geomechanical understanding of detrital materials, where deformation tends to be more progressive and less abrupt.

Figure 14 shows an example of historical data on detrital displacement rates.

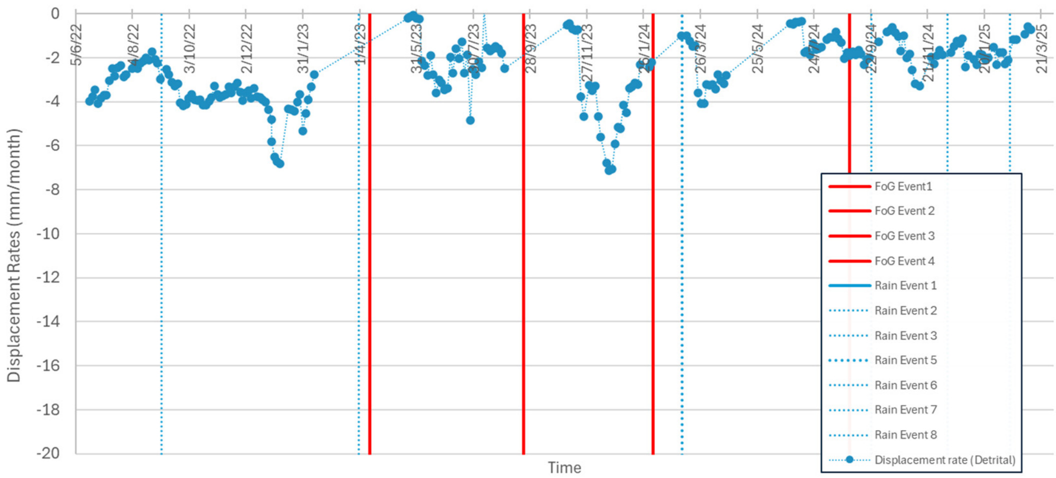

Figure 14 Historical data for detrital displacement rate

4.3.3 Stable materials and non-failure zones

Clusters 2 and 9 are primarily composed of areas with no recorded failure:

- Displacement rates in these clusters are generally low.
- Values exceeding 1.5 mm/month correspond to the 80th percentile, indicating that such rates are uncommon in stable conditions.

This insight is critical for defining a baseline of 'healthy' displacement behaviour in open pit slopes, helping to reduce false positives in early warning systems.

4.3.4 ALS1 post-failure behaviour

The ALS1 site, characterised by structural control and rainfall-induced movement, is represented in Cluster 6:

- displacement rates post-failure remain below 9 mm/month, even after more than a decade of monitoring.

- this value appears to represent a practical upper bound for residual movement in structurally controlled failures at ALS1.

Importantly, no additional failures have occurred in areas with displacement rates below this threshold, supporting its use as a post-failure stability marker.

4.4 Results for early warning markers

These findings demonstrate that SMA, when combined with clustering and statistical validation, can effectively distinguish between different failure stages and material behaviours. The results also provide a foundation for defining early warning indicators and post-failure thresholds tailored to specific geotechnical contexts as shown in Table 1

Table 1 Early warning markers

Material type	Pre-failure condition (early warning marker)	Post-failure condition (early warning marker for residual displacement)
	Parameter	**Parameter**
Detritals	>3 mm/month Consistent velocity over consecutive acquisitions For T = 24 hrs > 5 acquisitions For T = 72 hrs > 3 acquisitions For T = 120 hrs > 3 acquisitions Area size for analysis: (8,500 to 25,000 m²)	>8 mm/month Consistent velocity over consecutive acquisitions For T = 24 hrs > 5 acquisitions For T = 72 hrs > 3 acquisitions For T = 120 hrs > 3 acquisitions Area size for analysis: (8,500 to 25,000 m²)
ALS1 area	–	>10 mm/month Consistent velocity over consecutive acquisitions For T = 24 hrs > 5 acquisitions For T = 72 hrs > 3 acquisitions For T = 120 hrs > 3 acquisitions Area size for analysis: (8,500 to 25,000 m²)
All other materials	>1.5 mm/month Consistent velocity over consecutive acquisitions For T = 24 hrs > 5 acquisitions For T = 72 hrs > 3 acquisitions For T = 120 hrs > 3 acquisitions Area size for analysis: (8,500 to 25,000 m²)	–

This table provides early warning markers for interpreting SMA results in the context of early warning and post-failure assessment:

- Material-specific thresholds help distinguish between benign and concerning displacement behaviours.
- Area size is considered to avoid bias from spatial scale differences in SMA project configurations.
- Failure stage alignment with cluster membership validates the use of SMA for early detection and post-event monitoring.

5 Discussion

This study demonstrates that SMA, when combined with clustering and geotechnical classification, can effectively distinguish between failure stages and material behaviours in open pit slopes.

Key findings include:

- Material-specific displacement patterns: D-R contact materials under bedding control showed a clear transition from pre-failure to failure, with mean displacement rates increasing from ~1.4 to ~2.8 mm/month.
- Stable behaviour thresholds: clusters representing no-failure conditions (e.g. ACS3S, OC, S, W) consistently exhibited displacement rates below 1.5 mm/month, providing a baseline for 'healthy' slope movement.
- Post-failure stability: at ALS1, structurally controlled post-failure movement remained below 9 mm/month for over a decade, suggesting a practical upper bound for residual deformation.

These insights support the use of SMA as a proactive tool for early warning and post-failure assessment, particularly when integrated with material type and area size to refine interpretive thresholds.

Future work will expand this analysis by incorporating historical rainfall and blasting data to explore potential causal relationships with slope movement. Additionally, the methodology will be applied to other BHP sites in different geotechnical environments, such as iron oxide copper gold and copper porphyry deposits, to assess the applicability of SMA-based early warning indicators across diverse geological settings.

6 Conclusion

This study presents a comprehensive methodology for applying SMA to historical GBR (IDS ArcSAR radars) data in open pit mining environments. By combining time series feature extraction, hierarchical clustering, and geotechnical classification, the research identifies consistent displacement patterns associated with different failure mechanisms and material types.

Key contributions include:

- a robust analytical framework for detecting low-velocity slope movements using SMA
- validation of clustering results through statistical analysis and expert interpretation
- definition of material-specific early warning markers based on displacement rate thresholds
- integration of area size and failure stage to refine interpretive guidance.

The findings underscore the value of SMA as a complementary tool to real-time monitoring, particularly for identifying early-stage deformation that may not trigger conventional trigger action response plan thresholds. By embedding SMA insights into predictive monitoring systems, mine operators can enhance their ability to anticipate and mitigate slope failures, ultimately improving safety and operational resilience. The approach enables the development of material-specific early warning markers and interpretive rules that distinguish between benign and concerning movements. These insights support the creation of predictive monitoring workflows, offering a proactive framework for geotechnical risk management and enhancing decision-making in mine slope stability programs.

Acknowledgement

The authors would like to express their sincere gratitude to the WAIO Geotechnical Team for their invaluable contribution to this study. Their support in providing access to historical monitoring data, sharing site-specific insights, and offering expert geotechnical interpretation was instrumental in shaping the methodology and validating the results presented in this research.

References

Abrahams, G 2023, 'Safe management and optimisation of deforming pit walls', in PM Dight (ed.), *SSIM 2023: Third International Slope Stability in Mining Conference*, Australian Centre for Geomechanics, Perth, pp. 3–22, https://doi.org/10.36487/ACG_repo/2335_0.01

Crouse, RL & Wines, DR 2016, 'Cowal gold mine — documentation of slope deformations due to mining to final pit walls — a case history', in PM Dight (ed.), *APSSIM 2016: Proceedings of the First Asia Pacific Slope Stability in Mining Conference*, Australian Centre for Geomechanics, Perth, pp. 107–126, https://doi.org/10.36487/ACG_rep/1604_02_Crouse

Ebehardt, E, Stead, D, Stimpson, B & Read, R 1998, 'Identifying crack initiation and propagation thresholds in brittle rock', *Canadian Geotechnical Journal*, vol. 35, pp. 222–233.

Hutchinson, DJ 2023, 'Integrating monitoring data into risk assessment and management for rock slopes', in PM Dight (ed.), *SSIM 2023: Third International Slope Stability in Mining Conference*, Australian Centre for Geomechanics, Perth, pp. 55–64, https://doi.org/10.36487/ACG_repo/2335_0.04

IDS Georadar Division Mining 2018, *IBIS Slope Monitoring Focus on Slow Deformation Course*, Pisa, IDS Georadar, Pisa.

Leoni, L, Coli, N, Farina, P, Coppi, F, Michelini, A, Costa, TA, Costa, TAV & Costa, F 2015, 'On the use of ground-based synthetic aperture radar for long-term slope monitoring to support the mine geotechnical team', in PM Dight (ed.), *FMGM 2015: Proceedings of the Ninth Symposium on Field Measurements in Geomechanics*, Australian Centre for Geomechanics, Perth, pp. 789–796, https://doi.org/10.36487/ACG_rep/1508_58_Farina

Lowry, B, Gomez, F, Zhou, W & Mooney, M 2013, 'High resolution displacement monitoring of a slow velocity landslide using ground based radar interferometry', *Engineering Geology*, vol. 166, pp. 160–169, https://doi.org/10.1016/j.enggeo.2013.07.007

Michelini, A, Viviani, F & Mayer, L 2019, 'Introduction to IBIS-ArcSAR: a circular scanning GB-SAR system for deformation monitoring', *Proceedings of the 4th Joint International Symposium on Deformation Monitoring*.

Michelini, A, Coli, N, Coppi, F & Farina, P 2014, 'Advanced data processing of ground-based synthetic aperture radar for slope monitoring in open pit mines', *48th US Rock Mechanics/Geomechanics Symposium*, American Rock Mechanics Symposium, Alexandria.

Michelini, A, Coli, N, Coppi, F, Farina, P, Leoni, L, Costa, F, Costa, TA, Costa, T & Funaioli, G 2015, 'Advanced data processing of ground-based synthetic aperture radar for slope monitoring in open pit mines', *Proceedings of the 24th International Mining Congress of Turkey*, IMCET, pp. 420–442.

Morgan, JL, Colombo, D & Meloni, F 2019, 'InSAR tools for risk assessment over mine assets', in J Wesseloo (ed.), *MGR 2019: Proceedings of the First International Conference on Mining Geomechanical Risk, Australian Centre for Geomechanics*, Perth, pp. 159–170, https://doi.org/10.36487/ACG_rep/1905_06_Morgan

Murtagh, F & Legendre, P 2011, 'Ward's hierarchical clustering method: clustering criterion and agglomerative algorithm', *arXiv*, https://doi.org/10.48550/arXiv.1111.6285

Peryoga, T, Setiadi, B, Ursulic, A, Ziusudras, S & Earle, J 2023, 'Investigating potential long-term geotechnical risks with slow movement analysis', in PM Dight (ed.), *SSIM 2023: Third International Slope Stability in Mining Conference*, Australian Centre for Geomechanics, Perth, pp. 793–802, https://doi.org/10.36487/ACG_repo/2335_55

Read, PS 2009, *Guidelines for Open Pit Slope Design*, CSIRO Publishing, Melbourne.

Saunders, P, Nicoll, S & Christensen, C 2016, 'Slope stability radar alarm threshold validation at Telfer gold mine', in PM Dight (ed.), *APSSIM 2016: Proceedings of the First Asia Pacific Slope Stability in Mining Conference*, Australian Centre for Geomechanics, Perth, pp. 367–378, https://doi.org/10.36487/ACG_rep/1604_21_Saunders

Sharon, R & Eberhardt, E 2020, *Guidelines for Slope Performance Monitoring*, CSIRO Publishing, Melbourne.

Tovey, L, Dixon, R, Morgan, M & Shilov, E 2023, 'Rocks around the clock: a 24/7 approach to radar slope monitoring', in PM Dight (ed.), *SSIM 2023: Third International Slope Stability in Mining Conference*, Australian Centre for Geomechanics, Perth, pp. 741–756, https://doi.org/10.36487/ACG_repo/2335_51

Venter, J & Hamman, ECF 2019, 'A practical safety risk model for monitoring program design', in J Wesseloo (ed.), *MGR 2019: Proceedings of the First International Conference on Mining Geomechanical Risk, Australian Centre for Geomechanics*, Perth, pp. 195–204, https://doi.org/10.36487/ACG_rep/1905_09_Venter

Yang, H, Peng, J & Zhang, D 2011, *Slope of Large-scale Open-pit Mine Monitoring Deformations by Using Ground-Based Interferometry*, Department of Land Surveying and Geo-Informatics, Hong Kong.